

## Article

# Differential Expression Analysis of Blood MicroRNA in Identifying Potential Genes Relevant to Alzheimer's Disease Pathogenesis, Using an Integrated Bioinformatics and Machine Learning Approach

Mei Sze Tan <sup>1</sup>, Phaik-Leng Cheah <sup>2</sup>, Ai-Vyryn Chin <sup>3</sup>, Lai-Meng Looi <sup>2</sup> and Siow-Wee Chang <sup>1,4,\*</sup>

- <sup>1</sup> Bioinformatics Programme, Institute of Biological Sciences, Faculty of Science, Universiti Malaya, Kuala Lumpur 50603, Malaysia
- <sup>2</sup> Department of Pathology, Faculty of Medicine, Universiti Malaya, Kuala Lumpur 50603, Malaysia
- <sup>3</sup> Department of Medicine, Faculty of Medicine, Universiti Malaya, Kuala Lumpur 50603, Malaysia
- <sup>4</sup> Centre of Research in System Biology, Structural, Bioinformatics and Human Digital Imaging (CRYSTAL), Universiti Malaya, Kuala Lumpur 50603, Malaysia
- \* Correspondence: siowwee@um.edu.my or changsiowwee@gmail.com

**Abstract:** Alzheimer's disease (AD) is a neurodegenerative disease characterized by cognitive and functional impairment. Recent research has focused on the deregulation of microRNAs (miRNAs) in blood as the potential biomarkers for AD. As such, a differential expression analysis of miRNAs was conducted in this study using an integrated framework that utilized the advantages of statistical and machine learning approaches. Three miRNA candidates that showed the strongest significance and correlation with each other, namely hsa-miR-6501-5p, hsa-miR-4433b-5p, and hsa-miR-143-3p, were identified. The roles and functions of the identified differentiated miRNA candidates with AD development were verified by predicting their target mRNAs, and their networks of interaction in AD pathogenesis were investigated. Pathway analysis showed that the pathways involved in contributing to the development of AD included oxidative phosphorylation, mitochondrial dysfunction, and calcium-mediated signalling. This study supports evidence that the miRNA expression changes in AD and indicates the need for further study in this area.

**Keywords:** alzheimer's disease (AD); blood biomarkers; differential expression analysis; microRNAs



**Citation:** Tan, M.S.; Cheah, P.-L.; Chin, A.-V.; Looi, L.-M.; Chang, S.-W. Differential Expression Analysis of Blood MicroRNA in Identifying Potential Genes Relevant to Alzheimer's Disease Pathogenesis, Using an Integrated Bioinformatics and Machine Learning Approach. *Appl. Sci.* **2023**, *13*, 3071. <https://doi.org/10.3390/app13053071>

Academic Editor: Juan A. Gómez-Pulido

Received: 7 February 2023  
Revised: 24 February 2023  
Accepted: 24 February 2023  
Published: 27 February 2023



**Copyright:** © 2023 by the authors. Licensee MDPI, Basel, Switzerland. This article is an open access article distributed under the terms and conditions of the Creative Commons Attribution (CC BY) license (<https://creativecommons.org/licenses/by/4.0/>).

## 1. Introduction

Alzheimer's disease (AD) is the most common neurodegenerative disease that causes a dementing syndrome. It is clinically recognized by cognitive dysfunction, such as memory loss and behavioural changes that significantly impact functional ability [1]. AD is characterized pathologically by the abnormal accumulation of extracellular amyloid- $\beta$  peptide ( $A\beta$ ) plaques and intraneuronal neurofibrillary tangles (NFTs) composed of hyperphosphorylated tau protein in the brain [2,3]. The abnormal accumulation of these proteins is thought to lead sequentially to neuroinflammation, neuronal cell death, synaptic dysfunction, and finally, cognitive impairment [2]. AD appears to be genetically dichotomous, with rare mutations in amyloid precursor protein (*APP*), presenilin 1 (*PSEN1*), and presenilin 2 (*PSEN2*) associated with early-onset familial AD, and apolipoprotein E4 (*APOE4*) polymorphism associated with an increased risk of late-onset AD [4].

The diagnostic accuracy for AD has increased with the use of new neuroimaging modalities, such as amyloid or tau positron emission tomography (PET) scans, and the evaluation of biomarkers in cerebrospinal fluid (CSF), obtained via lumbar puncture [5]. However, these procedures are not suitable for the screening of normal populations as they are prohibitively expensive or invasive [5]. Hence, attention has been drawn to the

application of blood-based biomarkers, which is comparably more accessible and well-tolerated in regular clinical practice, to investigate and identify AD [5,6].

MicroRNAs (miRNAs), which circulate in the peripheral blood system, may be potential biomarkers for AD. The emergence of next-generation sequencing (NGS) technology, such as RNA sequencing (RNA-seq), of small RNAs enables the reading of thousands or millions of miRNA molecules, lending an understanding of their roles in neurodegenerative diseases for investigation. miRNAs are small (approx. 18–25 nucleotides long), non-coding RNA molecules that regulate posttranscriptional gene expression by binding to the 3'-untranslated regions of messenger RNAs (mRNAs). The changes in expression of a miRNA can repress the translation of many mRNAs (gene silencing), influencing the amounts and functions of numerous proteins. A miRNA can target multiple mRNAs, including mRNAs that exert contradicting effects within the same molecular pathway [7]. Several miRNAs that regulate the synthesis of activity-mediated proteins, affecting the underlying processes of cognitive function and disease risk/progression in AD, have previously been identified. miRNAs are abundant and stable in human bodily fluids, including the blood and the CSF, as compared to mRNAs, making miRNAs easier to evaluate and study [8].

Studies investigating the possibility of miRNAs as biomarkers for AD suggested that the dysregulation of miRNAs in blood may be able to reflect the pathological process of neuronal impairment that occurs in AD [5,6,9]. Aberrant expressions of miRNAs have been identified in AD, such as miR-101, miR-20a, and miR-17, which appear to negatively regulate the expression of *APP* [10,11]. Others, such as miR-22-3p and miR-340, were found to significantly alleviate  $A\beta$  levels in AD [11], whereas miR-107 levels were found to be negatively correlated with *APOE4* [10–13]. The suppression of miR-203 was also found to downregulate *APOE4* and tau in mice [11].

The analysis of complex and highly heterogeneous AD expression data requires strong computational power to untangle the network of interactions between the miRNAs and to select the most likely candidates with the highest sensitivity and specificity in relation to AD [14]. The “curse of dimensionality”, caused by the presence of large variables but a small sample size in a dataset, often poses the biggest challenge in the analysis of AD data [15]. The unbalanced ratio of the variables to the number of samples gives rise to the problem of overfitting and can increase false-positive results [14]. Although some statistical methods have been reported to perform well with such data comprising smaller sample sizes and high biological replicates [16,17], machine learning methods are deemed to be more reliable in solving data overfitting problems [18]. Feature-selection methods and cross-validation steps carried out during the analysis reportedly perform well at removing noise and outliers in the dataset, while avoiding overfitting caused by the high dimensionality of gene expression data [19].

In most conventional studies, the genes of interest are evaluated through their expression values in a case–control study, where a set of genes with expression that varied in one class, as compared to others, is selected. Numerous statistical models and tests have been developed with the aim of identifying the most significant set of candidates. However, statistical methods only focus on univariate comparison, and the importance of the gene–gene relationship is often neglected. On the contrary, other than predicting outcomes for classes to improve the performance of a model, machine learning can be used to select relevant features by looking into the intrinsic intervariable relationships of the genes.

In AD studies, machine learning methods have been applied to select differential miRNA biomarkers that exhibit similar structural and functional patterns [20]. The recent trend of machine learning in miRNA expression studies in AD mainly focuses on selecting a small set of miRNAs from a group of differentiated miRNAs to obtain more precise and reliable results of association [20,21].

The present case–control study focuses on investigating the differential miRNAs in the peripheral blood of Malaysian AD patients. The population in Malaysia is multi-ethnic and exposed to multicultural environments. Hence, this may result in differences not seen in the

findings of studies on monoethnic populations, such as Caucasian, African, and Chinese. The present study started with a data-integration framework that applied statistical and machine learning techniques to identifying potential miRNA candidates that demonstrate differential expression in AD patients as compared with controls. Problems caused by the high dimensionality of the dataset were minimized by conducting a two-step machine learning method in which supervised feature-selection and unsupervised clustering were carried out. In addition, the potential roles of the miRNA candidates in AD pathogenesis were correlated with the functions of their respective targeted mRNAs (genes) by carrying out miRNA target gene prediction. The pathways involved with the identified miRNAs and genes, together with their roles in AD, were discussed in an attempt to reach a more complete understanding of AD development.

The remainder of this paper is structured as follows: Section 2 discusses the existing methods used in the study of AD and the research gaps that need to be filled. Section 3 explains the materials used and the integration framework proposed in this study. Section 4 presents the results, and the findings are discussed in Section 5. Finally, conclusions are drawn and the challenges of this study are highlighted in Section 6.

## 2. Related Works

Previous studies have proposed the application of integrated statistical and machine learning models for the identification of potential miRNA candidates. Lugli et al. (2015) carried out a series of statistical and machine learning analyses to measure differential miRNAs and successfully identified seven miRNAs that showed significant differences in AD. The study compared the performance of several machine learning algorithms; however, the machine learning approaches were not used as a part of the differential miRNA expression analysis, but rather to evaluate how robust each algorithm is [22]. Furthermore, a study of 14 miRNAs with differential expression in an AD group, as compared to normal controls, was conducted [23]. Similar to aforementioned studies, the proposed methods of statistical and machine learning approaches were applied here to carry out different tasks in our study: statistical methods for differential miRNA expression and machine learning for prediction performance.

The lack of the utilization of machine learning techniques in the analysis of differential miRNA expression data, especially in AD-related fields, represents a research gap that needs to be addressed.

## 3. Methods and Materials

### 3.1. Subjects

A total of 12 subjects were recruited from the Memory Clinic and the Geriatric Clinic, University of Malaya Medical Centre (UMMC), Kuala Lumpur, Malaysia, for the present study. Blood samples were collected from the subjects, including eight patients diagnosed with AD and four normal controls. All of the subjects were over 65 years of age at the time of recruitment and had been assessed by a geriatrician with experience in dementia care. The selection criteria used in recruiting the subjects are included in the Supplementary Materials, Table S1. The subjects' details and the corresponding sample IDs used in this study are included in the Supplementary Materials, Table S2. The study protocol was approved by the Medical Research Ethics Committee, UMMC, with the approval number 2020114-9193.

The study was carried out according to the framework illustrated in Figure 1.

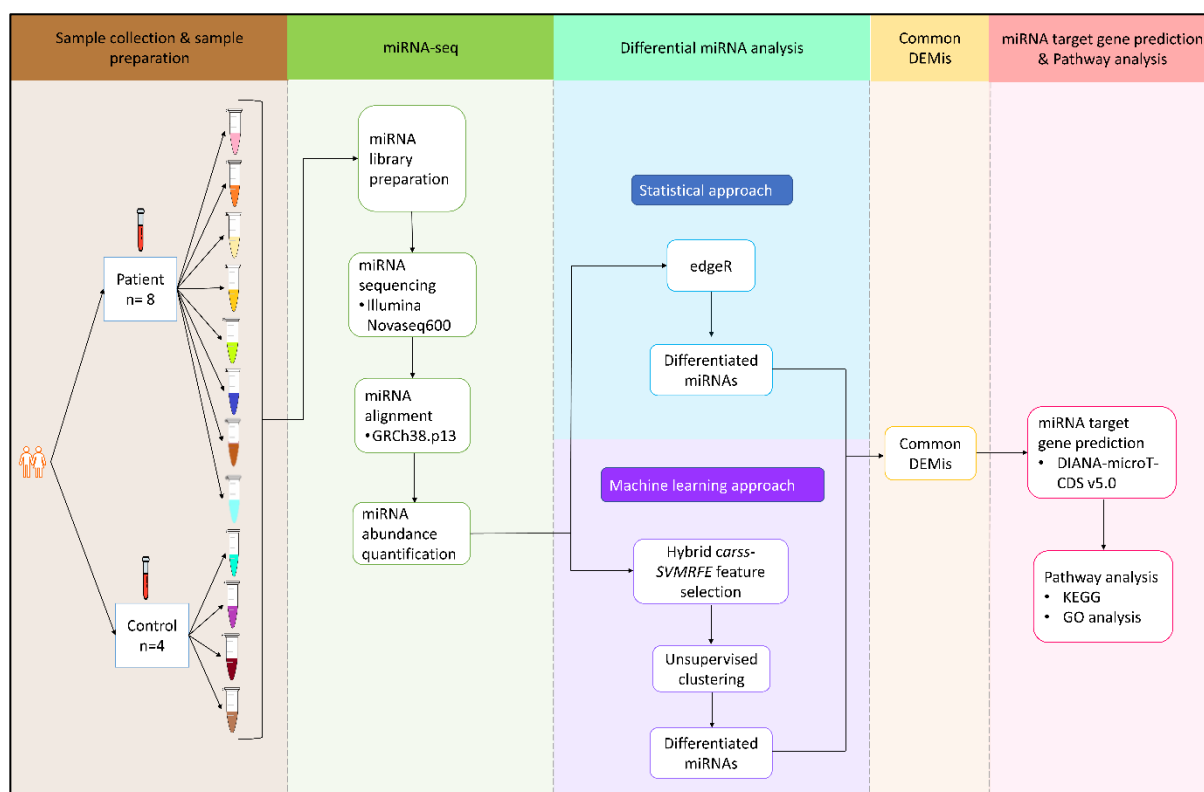


**Figure 1.** The framework for the differential expression analysis of miRNA in the blood of AD patients and that of normal controls. miRNA sequencing was conducted on the samples after appropriate preparation. The raw count data were analysed using bioinformatics. Differential miRNA expression analysis was carried out using two independent approaches, i.e., statistical and machine learning. Differentially expressed miRNAs (DEMIs) were subjected to miRNA target gene prediction, followed by the evaluation of enriched pathways.

### 3.2. Sample Preparation

A quantity of 6 ml of blood was collected from each subject in a BD Vacutainer EDTA blood collection tube. A series of routine investigations, extraction, and centrifuging were conducted, and the samples were stored at  $-80^{\circ}\text{C}$  until further processing. The details of the procedure are listed in the Supplementary Materials. The DNA and other blood contaminants in the samples were eliminated, and the quantity and purity of the RNA samples were measured using Nanodrop.

### 3.3. Small RNA-Sequencing Analysis

Small RNA libraries were constructed from the RNA samples using a NEXTFlex Illumina Small RNA-seq Kit v3 (Bioo Scientific, Austin, TX, USA), following the manufacturer's protocol. The libraries were loaded and sequenced on the Illumina NovaSeq 6000, and more than 10 M (1.5 Gb) reads were obtained from each library. The raw reads were first quality-checked, and low-quality bases were trimmed from the 3' end. Subsequently, the reads were dynamically trimmed for an adapter sequence by using cutadapt [24]. Clean reads were then mapped against the reference genome (*H\_sapien*) using Bowtie [25]. The matched reads were aligned to identify mature miRNAs in miRbase v22. The count data were used for further bioinformatics analysis.

### 3.4. Integrative Statistical and Machine Learning Analysis

#### 3.4.1. Differential Expression Analysis

(i) Statistical approach: EdgeR

Raw counts from the miRNA sequencing dataset were filtered to exclude miRNAs with low expressed counts (<10 counts for every sample). The resulting counts were first scaled according to the library size, followed by normalization using a method known as the trimmed mean of M-values (TMM) [26]. The normalization was based on the log-expression ratio of the read count data [26]. Differential miRNA expression analysis was carried out to compare the AD and control groups, based on a linear model generalized by negative binomial distribution in edgeR [27]. A  $p$ -value of <0.05 was considered significant and was applied as the threshold for selecting the top differentially expressed miRNA (DEMi) candidates. DEMi candidates with  $\log_2$  fold-change (FC) values that were >0.5 were considered as upregulated, and those with  $\log_2$ FC < -0.5 were considered as downregulated.

#### (ii) Machine learning approach

##### Step 1: Hybrid *carss*-*SVMRFE* feature-selection

Feature-selection was performed using the normalized miRNA dataset (with low-quality reads filtered out) so as to filter out the uninformative genes and to select a subset of genes with the most relevant features. The input expression data were first normalized and  $\log_2$ -transformed according to the trimmed mean of M-values (TMM) in edgeR, which minimized the difference in the miRNAs with low expression counts, creating a fitted dispersion with a weaker bias effect.

The present study implemented supervised feature-selection using a hybrid filter-wrapper approach based on the absolute correlation-adjusted regression survival scores (*carss*) and multiple support vector machine recursive feature elimination (*MSVM-RFE*) in packages *mlr3* and *e1071*, R [28,29].

First, the filter method *carss* was used to select informative variables based on the measurements of the correlation between the “decorrelated” variables, while considering the target outcome (AD/normal control). Subsequently, *MSVM-RFE* was conducted as the wrapper method to select miRNA subsets that could improve the results for subsequent analysis. A sequential backward elimination procedure was applied in *MSVM-RFE* recursively ( $k = 5$ ), and feature-ranking scores were calculated in each fold. The average ranking was computed for each feature, and the best feature subset was selected. At the end of this step, the top 50 ranked features (miRNAs) were selected, and those proceeded to the next step.

##### Step 2: Principal component analysis (PCA) with self-organizing map (SOM)

Next, SOM [30] was performed using the top 50 miRNAs that were selected in Step 1. SOM is an unsupervised clustering method of neural networks which groups and captures the input pattern of the gene expression data in terms of learning rules and then organizes it to reflect the clustering in the final layer [31]. Therefore, the output of a SOM contains clusters, with each cluster containing features of similar characteristics, and the high dimensionality of the data is reduced. In this study, a SOM with a map size of  $2 \times 2$ , with hexagonal topology, was applied. Hierarchical clustering (HC) was then applied to the resulting SOM cluster to further define the clusters. The miRNAs were clustered according to their expression values, without the predefined knowledge of the dependent class labels [32]. The outcomes were visualized using PCA to observe the gene expression patterns of the clusters resulting from the SOM. PCA is a method that has the ability to reduce the dimensionality of the data while compressing the complexity of the data [33,34]. This technique was applied in this study to improve the interpretability of the SOM results.

#### 3.4.2. miRNA Target Gene Prediction

miRNA target gene prediction was performed using DIANA-microT-CDS v5.0 [35]. The prediction threshold was set to 0.7 (sensitive), and the keyword “Alzheimer” was inserted into the queries to identify potential gene targets that are related to AD.

#### 3.4.3. miRNA Pathway and Gene Ontology (GO) Analysis

By utilizing the target genes predicted in the previous step, DIANA-miRPath v3.0 [36] was used to carry out miRNA pathway analysis to discover the possible pathways involved

in AD pathogenesis. The target genes were enriched with KEGG pathway [37] and GO analysis [38]. GO terms, including the biological process, the molecular functions, and the cellular functions, were investigated. The significant threshold of  $p$ -value  $<0.05$  was corrected according to the false discovery rate (FDR). Additionally, the species “Human” was specified in the query. Significant and common pathways were selected using gene union tools. Furthermore, networks showing the interactions between the miRNAs and the target genes in specific pathways were depicted using Cytoscape [39].

#### 4. Results

Unfortunately, one sample (AD 8) failed during the construction of the small RNA libraries and had to be excluded as analysis of the miRNA concentration of this sample by the Small RNA bioanalyzer produced an inconclusive outcome, thus leaving a total of 11 samples to be entered into the study. As a result, a total of 420 mature miRNAs were included in the analysis after reads of a low quality were removed.

##### 4.1. Statistical Approach: edgeR

In the differential miRNA analysis using edgeR, 12 DEMi candidates (5 upregulated and 7 downregulated) were identified between the AD and normal control groups, with a significant threshold  $p$ -value of  $<0.05$  (Table 1).

**Table 1.** DEMi candidates selected using edgeR.

DEMi	Log2FC	$p$ -Value	Regulation
hsa-miR-941	0.752891	0.020286	Up
hsa-miR-1273c	0.72872	0.016058	Up
hsa-miR-150-5p	0.685625	0.049536	Up
hsa-miR-10a-5p	0.597925	0.023684	Up
hsa-miR-9-5p	0.563954	0.011416	Up
hsa-miR-1307-3p	−0.59803	0.024833	Down
hsa-miR-877-5p	−0.61671	0.048433	Down
hsa-miR-4433b-5p	−0.67039	0.036891	Down
hsa-miR-143-3p	−0.69404	0.048802	Down
hsa-miR-1296-5p	−0.85825	0.018019	Down
hsa-miR-5100	−1.21725	0.046714	Down
hsa-miR-6501-5p	−1.34159	0.003957	Down

##### 4.2. Machine Learning Approach

The original, mature miRNAs ( $n = 420$ ) were first filtered using a supervised hybrid filter-wrapper approach as the feature-selection method. As the result, top 50 ranked miRNAs were identified, and an unsupervised machine learning approach using SOM was performed.

The input data were presented in the  $2 \times 2$  feature output space, which consisted of four neurons in total. A total of 50 features of the data were clustered into 4 neurons. The mean distance was calculated based on the position of each neuron. Following that, additional subclustering was subsequently carried out, using HC on the  $2 \times 2$  feature output space to split the four neurons into two clusters, as shown in Figure 2.

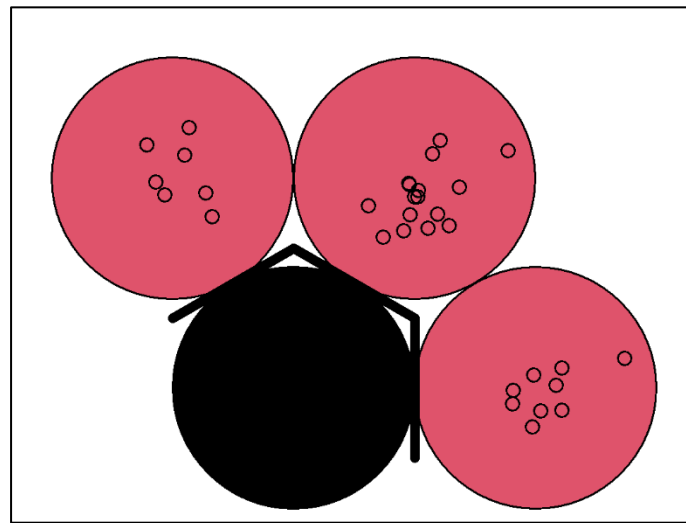


**Figure 2.** Clustering of SOM neurons using HC.

Figure 2 illustrates the subclusters of the four neurons generated in SOM. Of the four neurons, three had higher connectivity with one another (pink), which indicated that these neurons were located in the same cluster. In contrast, the remaining cluster contained only one neuron (black).

Next, the result was visualized using PCA to produce a more interpretable view of the miRNA clustering. Figure 3A shows the distribution of the miRNAs in the two clusters, as extended from Figure 2. Figure 3B shows the distribution pattern of the samples, indicated by the pointing of the arrows that originate from the centre point. All of the AD samples were located on the right side of the plot, indicating higher values in these samples. Corresponding to the pattern of miRNA clustering in Figure 3A, the miRNAs in SOM cluster 1 (red dots) showed a similar distribution to the AD cohorts in Figure 3B. Hence, the member miRNAs in SOM cluster 1 in Figure 3A were identified, and 24 miRNAs were selected as DEMi candidates.

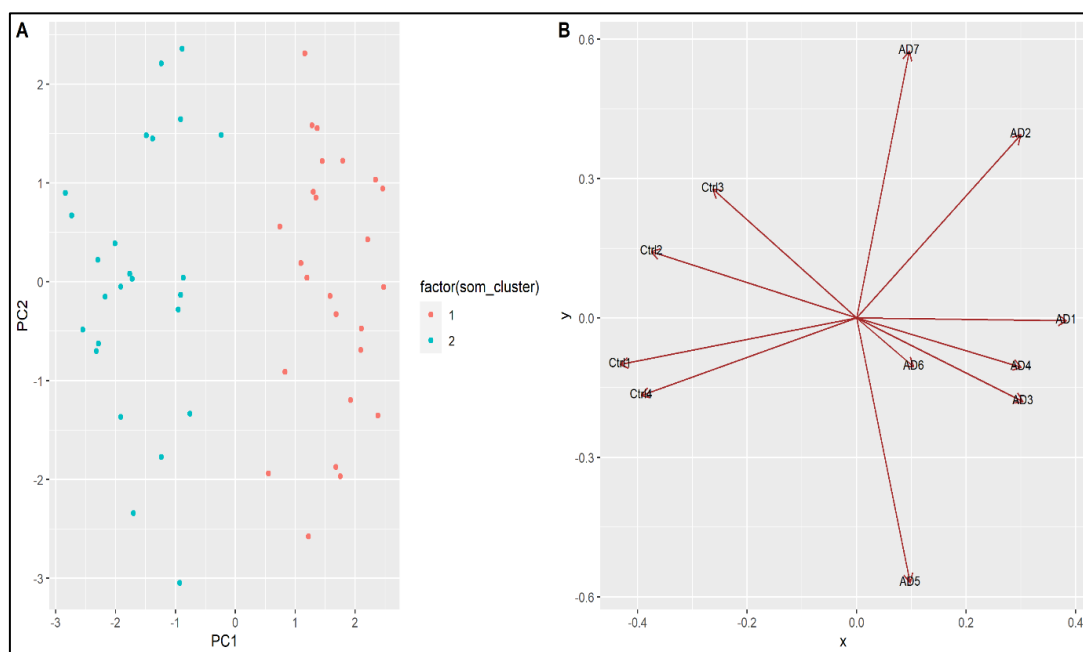


**Figure 3.** PCA plot of (A) clusters of top 50 ranked miRNAs based on SOM; (B) sample distribution corresponding to PCA: x-axis = PC1, y-axis = PC2.

#### 4.3. Integrated Bioinformatics and Machine Learning Approach

The DEMi candidates identified using the machine learning approach were compared with the DEMi candidates identified using edgeR so as to identify common DEMis. A Venn diagram of this comparison is shown in Figure 4.



**Figure 4.** Venn diagram of the DEMi candidates identified using edgeR and the machine learning approach.

Five common DEMis (hsa-miR-6501-5p, hsa-miR-1296-5p, hsa-miR-1307-3p, hsa-miR-4433b-5p, and hsa-miR-143-3p) were identified in this study.

#### 4.4. Target Gene Prediction

Target gene prediction, which was carried out subsequently, identified the mRNAs associated with the five common DEMis. Notably, only three DEMis, hsa-miR-6501-5p, hsa-miR-4433b-5p, and hsa-miR-143-3p, were predicted to be related to AD and thus were selected as the DEMi signatures for this study (Table 2).

**Table 2.** DEMis and the predicted target genes related to AD.

DEMi	Gene ID	Gene Name	miTG Score
hsa-miR-6501-5p	ENSG00000124172	<i>ATP5E</i>	0.824031785
	ENSG00000138814	<i>PPP3CA</i>	0.793189081
hsa-miR-4433b-5p	ENSG00000161509	<i>GRIN2C</i>	0.754847813
	ENSG00000160014	<i>CALM3</i>	0.746931533
	ENSG00000162736	<i>NCSTN</i>	0.720055687
hsa-miR-143-3p	ENSG00000273079	<i>GRIN2B</i>	0.932644441
	ENSG00000172071	<i>EIF2AK3</i>	0.898086248
	ENSG00000147684	<i>NDUFB9</i>	0.852775513
	ENSG00000139180	<i>NDUFA9</i>	0.84781014
	ENSG00000080815	<i>PSEN1</i>	0.825585469
	ENSG00000100030	<i>MAPK1</i>	0.756048436
	ENSG00000023228	<i>NDUFS1</i>	0.751173742
	ENSG00000198838	<i>RYR3</i>	0.744614559
	ENSG00000186318	<i>BACE1</i>	0.739327029
ENSG00000131143	<i>COX4I</i>	0.736374347	

#### 4.5. miRNA Pathway and Gene Ontology (GO) Analysis

Next, KEGG pathways involved with the identified AD-related target genes were identified (Table 3). Interaction networks of the three identified DEMi signatures with

the target genes and their corresponding pathways are illustrated in Figure 5. The results indicate that the significantly enriched pathways of the three DEMi signatures and their respective target genes are involved in six pathways, which are the AD, oxidative phosphorylation, circadian entrainment, amphetamine addiction, long-term potentiation, and oxytocin pathways.

**Table 3.** KEGG pathways associated with the DEMi signatures and the respective target genes.

KEGG Pathway	<i>p</i> -Value	DEMi Involved	Gene Involved
Alzheimer's disease	$1.58 \times 10^{-10}$	hsa-miR-6501-5p	<i>ATP5E</i> <i>PPP3CA</i>
		hsa-miR-4433b-5p	<i>GRIN2C</i> <i>CALM3</i> <i>NCSTN</i>
		hsa-miR-143-3p	<i>EIF2AK3</i> <i>NDUFB9</i> <i>NDUFA9</i> <i>PSEN1</i> <i>MAPK1</i> <i>NDUFS1</i> <i>RYR3</i> <i>BACE1</i> <i>COX4I1</i>
Oxidative phosphorylation	$9.67 \times 10^{-6}$	hsa-miR-6501-5p	<i>ATP5E</i> <i>NDUFB9</i>
		hsa-miR-143-3p	<i>NDUFA9</i> <i>NDUFS1</i> <i>COX4I1</i>
Circadian entrainment	0.023972099	hsa-miR-4433b-5p	<i>GRIN2C</i> <i>CALM3</i>
		hsa-miR-143-3p	<i>MAPK1</i> <i>RYR3</i>
Amphetamine addiction	0.023972099	hsa-miR-6501-5p	<i>PPP3CA</i>
		hsa-miR-4433b-5p	<i>GRIN2C</i> <i>CALM3</i>
Long-term potentiation	0.023972099	hsa-miR-6501-5p	<i>PPP3CA</i>
		hsa-miR-4433b-5p	<i>GRIN2C</i> <i>CALM3</i>
		hsa-miR-143-3p	<i>MAPK1</i>
Oxytocin signalling pathway	0.023972099	hsa-miR-6501-5p	<i>PPP3CA</i>
		hsa-miR-4433b-5p	<i>CALM3</i>
		hsa-miR-143-3p	<i>MAPK1</i> <i>RYR3</i>

In the GO analysis, 12 significant enriched GO terms were identified (Table 4), with the suggestion that the DEMi signatures and target genes were mainly related to the generation of precursor metabolites and energy, mitochondrion, calcium-mediated signalling, and protein metabolic processes. Notably, hsa-miR-4433b-5p and hsa-miR143-3p showed common enrichment to the terms relating to  $A\beta$ , which is one of the important pathological indicators for AD. The interaction networks of the three identified DEMi signatures with the target genes and their corresponding pathways are illustrated in Figure 6.

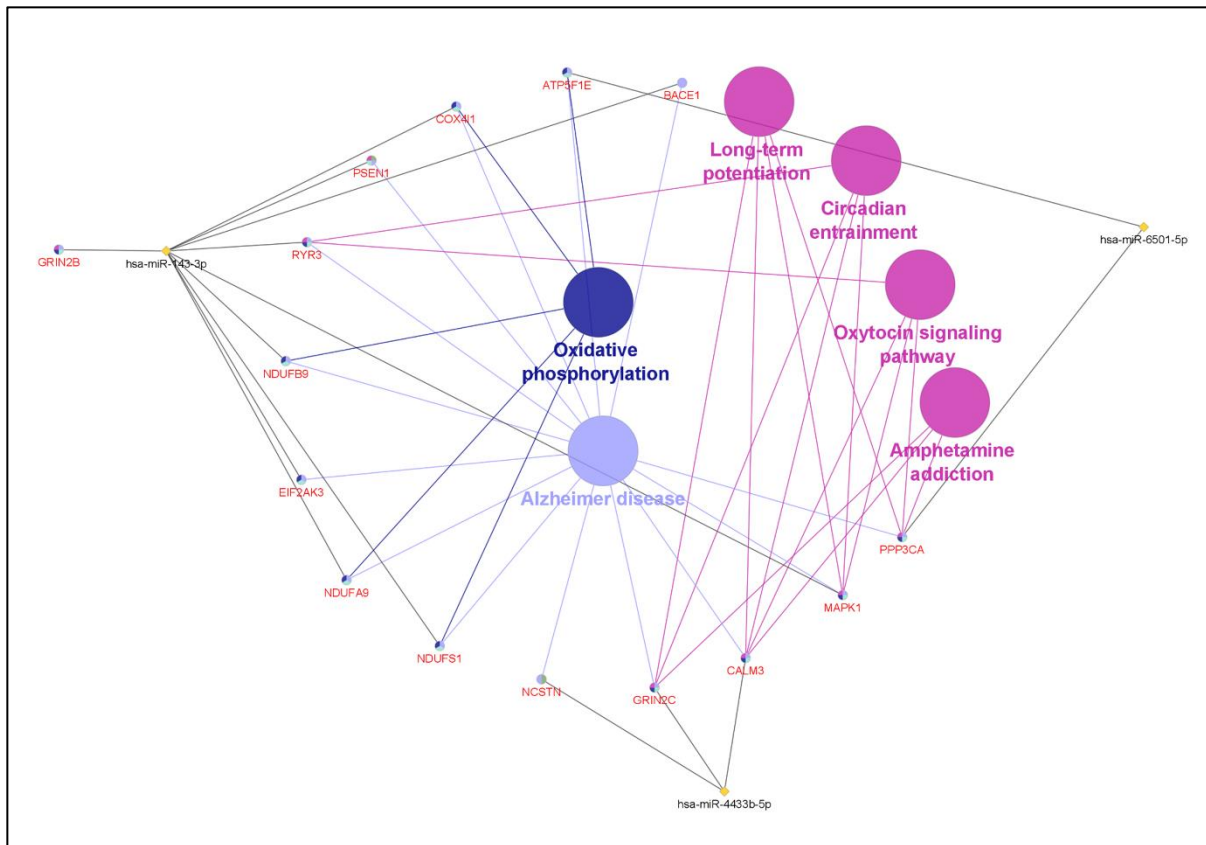


**Figure 5.** DEMi signatures and target genes enriched in KEGG pathways. Enriched pathways are indicated by the nodes, and the interactions between the pathways and genes are represented by lines. The different colours of the nodes depict the different functional groups of the pathways.

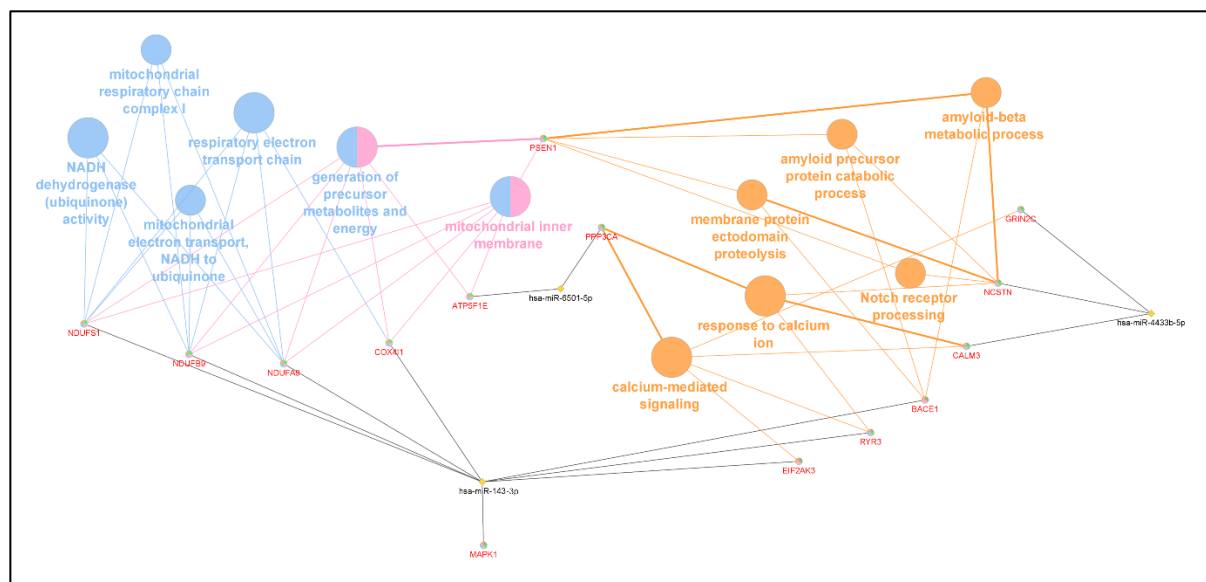


**Figure 6.** DEMi signatures and target genes enriched with GO terms. Enriched GO terms are indicated by the nodes, and the interactions between the terms and genes are represented using lines. The different colours of the nodes depict the different functional groups of the GO terms.

**Table 4.** GO terms associated with the miRNAs and the respective target genes.

GO Category	<i>p</i> -Value	DEMi Involved	Genes Involved
respiratory electron transport chain	$1.19 \times 10^{-5}$	hsa-miR-6501-5p	<i>ATP5E</i> <i>NDUFB9</i> <i>NDUFA9</i> <i>NDUFS1</i>
		hsa-miR-143-3p	<i>COX4I1</i>
generation of precursor metabolites and energy	$3.03 \times 10^{-5}$	hsa-miR-6501-5p	<i>ATP5E</i>
		hsa-miR-4433b-5p	<i>CALM3</i>
		hsa-miR-143-3p	<i>NDUFB9</i> <i>NDUFA9</i> <i>NDUFS1</i> <i>COX4I1</i>
beta-amyloid metabolic process	0.001017955	hsa-miR-4433b-5p	<i>NCSTN</i>
		hsa-miR-143-3p	<i>PSEN1</i> <i>BACE1</i>
calcium-mediated signalling	0.001521237	hsa-miR-6501-5p	<i>PPP3CA</i>
		hsa-miR-4433b-5p	<i>CALM3</i>
		hsa-miR-143-3p	<i>EIF2AK3</i>
membrane protein ectodomain proteolysis	0.002220614	hsa-miR-143-3p	<i>PSEN1</i> <i>BACE1</i>
		hsa-miR-4433b-5p	<i>NCSTN</i>
mitochondrial inner membrane	0.005473536	hsa-miR-143-3p	<i>NDUFB9</i> <i>NDUFA9</i> <i>PSEN1</i> <i>NDUFS1</i> <i>COX4I1</i>
mitochondrial electron transport, NADH to ubiquinone	0.005473536	hsa-miR-143-3p	<i>NDUFB9</i> <i>NDUFA9</i> <i>NDUFS1</i>
NADH dehydrogenase (ubiquinone) activity	0.01130008	hsa-miR-143-3p	<i>NDUFB9</i> <i>NDUFA9</i> <i>NDUFS1</i>
mitochondrial respiratory chain complex I	0.01133565	hsa-miR-143-3p	<i>NDUFB9</i> <i>NDUFA9</i> <i>NDUFS1</i>
amyloid precursor protein catabolic process	0.0124875	hsa-miR-4433b-5p	<i>NCSTN</i>
		hsa-miR-143-3p	<i>PSEN1</i>
Notch-receptor processing	0.01577116	hsa-miR-4433b-5p	<i>NCSTN</i>
		hsa-miR-143-3p	<i>PSEN1</i>
response to calcium ion	0.01746326	hsa-miR-6501-5p	<i>PPP3CA</i>
		hsa-miR-4433b-5p	<i>CALM3</i>

Although gene *GRIN2B* was selected as one of the target genes for hsa-miR-143-3p in relation to AD, it was identified as being involved in neither the pathways, nor in the GO analysis. Similarly, a family member of *GRIN2B*, named *GRIN2C*, was identified in the KEGG pathway analysis but not in the GO analysis.

## 5. Discussion

The present study aimed to provide new insight into AD by studying miRNAs in Malaysians. Although AD is the most common type of dementia and is known to have

a strong association with the accumulation of  $A\beta$  and phosphorylated tau protein, the mechanisms involved in the pathogenesis of this disease are still uncertain and may be related to environmental, genetic, cultural, and other factors [2,4].

The five common miRNAs identified (hsa-miR-6501-5p, hsa-miR-1296-5p, hsa-miR-1307-3p, hsa-miR-4433b-5p, and hsa-miR-143-3p), when the DEMis, using statistical (edgeR) and machine learning approaches were compared, were downregulated DEMis in edgeR (Table 1). Downregulated miRNAs often cause the upregulation of target genes, and vice versa, and as such, this finding may be related to the roles played by the miRNAs in suppressing mRNA expression [26].

Among these five commonly identified DEMis, only three DEMis (hsa-miR-6501-5p, hsa-miR-4433b-5p, and hsa-miR-143-3p) were predicted to have target genes related to AD (see Table 2). Although the role of hsa-miR-6501-5p in AD is ambiguous, two target genes, *ATP5E* and *PPP3CA*, were predicted to be involved in AD-related pathways.

Hsa-miR-4433, of which hsa-miR-4433b-5p is a member, has been identified as regulating glial cells and neuroimmune systems, indicating the participation of this miRNA in neurodegenerative disease [40]. Hsa-miR-4433b-5p has also previously been associated with neurodegenerative diseases such as AD, Parkinson's disease (PD), and frontotemporal dementia (FTD) [41]. It is negatively correlated with lipids, where the formation of  $A\beta$  is involved in the cholesterol-metabolism regulation pathway [42]. In relation to AD, *GRIN2C*, *CALM3*, and *NCSTN* are downstream target genes of hsa-miR-4433b-5p.

Hsa-miR-143-3p has been suggested as a possible AD biomarker in review studies [43,44]. In our study, hsa-miR-143-3p was downregulated in the plasma of AD patients, which is consistent with the findings seen in another study using an AD cell-culturing model [45]. The overexpression of hsa-miR-143-3p has been observed to attenuate tau phosphorylation, decrease *APP* levels, and reduce  $A\beta$  accumulation [45]. Another AD cell model, however, found that the inhibition of hsa-miR-143-3p fostered neuronal survival and indirectly slowed down AD progression, which was an upregulated expression in the serum of AD patients [43]. That finding was contradictory to that of the present study, which is probably due to the different sample types used. Several genes that are related to AD, those being *GRIN2B*, *EIF2AK3*, *NDUFB9*, *NDUFA9*, *PSEN1*, *MAPK1*, *NDUFS1*, *RYR3*, *BACE1*, and *COX4I1*, have been identified as the target genes for hsa-miR-143-3p.

The roles and functions of the target genes in AD pathogenesis are summarized in Table 5.

**Table 5.** List of target genes and their roles and functions as related to AD.

Gene	Roles and Functions as Related to AD
<b>ATP synthase F1 subunit epsilon (<i>ATP5E</i>)</b>	<ul style="list-style-type: none"> <li>• A mitochondrial-encoded oxidative phosphorylation (OXPHOS) gene [46].</li> <li>• OXPHOS dysfunction increases the level of reactive oxygen species (ROS) and oxidative stress, which subsequently leads to neuronal damage in the AD brain [47].</li> </ul>
<b>Protein phosphatase 3 catalytic subunit alpha (<i>PPP3CA</i>)</b>	<ul style="list-style-type: none"> <li>• A catalytic subunit of calcineurin, which is involved in the calcium signalling and inflammatory pathways related to AD [48].</li> <li>• Dysregulation of <i>PPP3CA</i> was observed in the AD brain through its involvement with oxidative stress and pathological cellular dysfunction losses [48,49].</li> </ul>
<b>Glutamate Ionotropic Receptor NMDA Type Subunit 2C (<i>GRIN2C</i>)</b>	<ul style="list-style-type: none"> <li>• Takes part in glutamate-mediated neurotoxicity, which stimulates the progressive decline of cognitive function in AD patients [50].</li> </ul>
<b>Calmodulin 3 (<i>CALM3</i>)</b>	<ul style="list-style-type: none"> <li>• An indicator for calcium signalling dysfunction, where lower expressions were detected in AD patients as compared to normal controls [51,52].</li> </ul>

Table 5. Cont.

Gene	Roles and Functions as Related to AD
Nicastrin ( <i>NCSTN</i> )	<ul style="list-style-type: none"> <li>Nicastrin is one of the subunits of <math>\gamma</math>-secretase that plays an important role in the amyloidogenic pathways of AD pathogenesis [53].</li> <li>The inactivation of <i>NCSTN</i> restricts <math>A\beta</math> production and subsequently inhibits neurodegeneration [53,54].</li> </ul>
Glutamate Ionotropic Receptor NMDA Type Subunit 2B ( <i>GRIN2B</i> )	<ul style="list-style-type: none"> <li>Expresses in the brain regions that are predominantly affected in AD [55].</li> <li>Involved in synaptic functioning, where its dysfunction leads to neuronal damage and cognitive impairment [55].</li> </ul>
Eukaryotic translation initiation factor 2 alpha kinase 3 ( <i>EIF2AK3</i> )	<ul style="list-style-type: none"> <li>Encodes for PERK protein, which is involved in cognitive activities such as learning and memory [56].</li> <li>Overexpression of <i>EIF2AK3</i> induces tau phosphorylation and promotes amyloidogenesis [56].</li> <li>Interacts with the strongest genetic factor of AD, APOE4 [56,57].</li> </ul>
NADH:ubiquinone oxidoreductase subunit B9 ( <i>NDUFB9</i> )	<ul style="list-style-type: none"> <li>An OXPHOS gene [46].</li> <li>Involved in the oxidative phosphorylation pathway in AD [58].</li> </ul>
NADH:ubiquinone oxidoreductase subunit A9 ( <i>NDUFA9</i> )	<ul style="list-style-type: none"> <li>An OXPHOS gene [46].</li> <li>Involved in mitochondrial failure, leading to <math>A\beta</math> accumulation [59].</li> </ul>
Presenilin 1 ( <i>PSEN1</i> )	<ul style="list-style-type: none"> <li>Most prevalent genetic variant of AD [59,60].</li> <li>Encodes protein presenilin 1, which is one of the subunits of <math>\gamma</math>-secretase that plays an important role in the amyloidogenic pathway of AD pathogenesis [60,61].</li> <li>Exacerbates the production of <math>A\beta</math> in AD pathogenesis [61].</li> </ul>
Mitogen-activated protein kinase 1 ( <i>MAPK1</i> )	<ul style="list-style-type: none"> <li>Takes part in cellular signal transduction [62].</li> <li><math>A\beta</math> induces the elevation of <i>MAPK1</i> expression, elevates tau phosphorylation, exacerbates the amyloidogenic pathway, and aggravates AD development [62,63].</li> </ul>
NADH:ubiquinone oxidoreductase subunit S1 ( <i>NDUFS1</i> )	<ul style="list-style-type: none"> <li>An OXPHOS gene [46,64].</li> <li>Involved in mitochondrial energy metabolism; however, its main function remains unknown [64,65].</li> </ul>
Ryanodine receptor 3 ( <i>RYR3</i> )	<ul style="list-style-type: none"> <li>Releases stored calcium ions into the extracellular space [66].</li> <li>The deposition of <math>A\beta</math> causes the increase of <i>RYR3</i> expression [66].</li> <li>The upregulation of <i>RYR3</i> may form a protection for the neurons and against the impact of <math>A\beta</math> in the late stage of AD [67,68].</li> </ul>
$\beta$ -secretase cleaving enzyme 1 ( <i>BACE1</i> )	<ul style="list-style-type: none"> <li>Responsible for <math>\beta</math>-secretase activity in the amyloidogenic pathway, which initiates the generation of <math>A\beta</math> [69].</li> <li>Shows high expression in AD patients as compared to normal controls, including in the plasma [70].</li> <li>The inhibition of <i>BACE1</i> serves as the target for the study of AD drug candidates [71].</li> </ul>
Cytochrome c oxidase subunit 4I1 ( <i>COX4I1</i> )	<ul style="list-style-type: none"> <li>Involved in the mitochondrion electron transport chain, a crucial mechanism in cellular metabolism and the electron transport chain [72].</li> <li>The cleavage of APOE<math>\epsilon</math>4 inhibits the <i>COX</i> gene, leading to mitochondrial dysfunction [73].</li> <li><i>COX4I1</i> showed significant downregulation in AD patients [72].</li> </ul>

The roles and functions of the DEMi signatures and their respective target genes further corroborate the results of the KEGG pathway and GO analysis (see Tables 3 and 4). Pathways related to oxidative phosphorylation, mitochondrial dysfunction, and calcium-mediated signalling are particularly highlighted in the present study. The interaction of the genes is demonstrated in Figure 7.

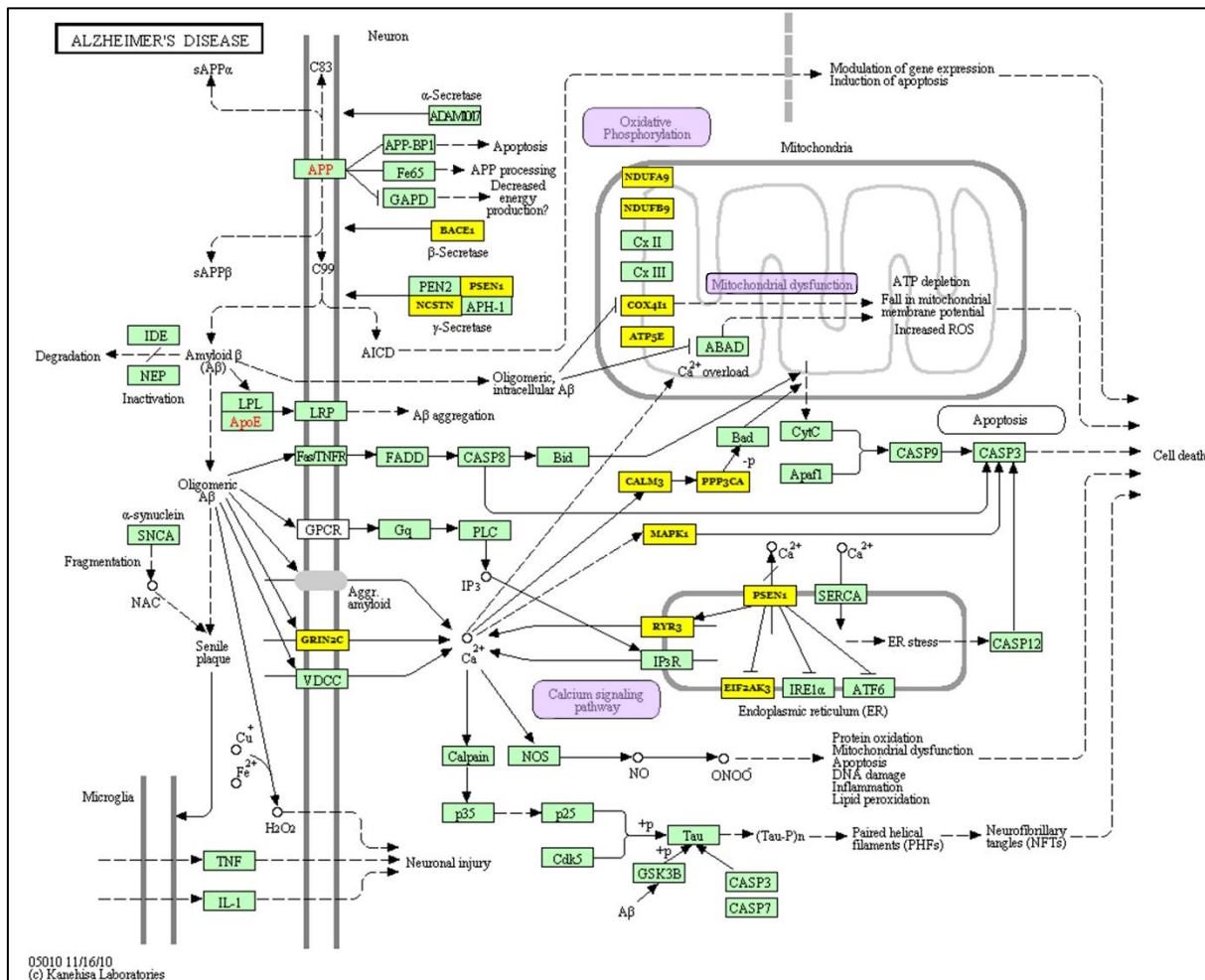


**Figure 7.** KEGG Alzheimer’s disease pathway (hsa05010): The selected target genes are highlighted by yellow boxes. The genes involved in oxidative phosphorylation, mitochondrial dysfunction, and the calcium signalling pathways are indicated by purple boxes. The gene *GRIN2B* was not identified as being involved in this pathway and is therefore excluded from the figure.

Defects in oxidative phosphorylation, mitochondrial mechanisms, and calcium signalling are interconnected in a cascade sequence and ultimately lead to neurodegeneration in AD. Failure in oxidative phosphorylation causes the deregulation of ATP-synthase activities in mitochondria and contributes to the elevation of oxidative stress and cell death of neuronal mechanisms [74,75]. Damage to mitochondrial function has been postulated as being the fundamental feature of AD pathogenesis. The alteration of mitochondrial mechanisms causes the impairment of energy metabolism in AD, especially in the brain, which consumes a high level of energy, and eventually leads to neuronal cell death [76,77]. Dysregulation of calcium homeostasis is closely connected to Aβ in AD. Aβ has been reported to trigger intracellular calcium deregulation, which probably elevates reactive oxygen species (ROS), suppresses ATP production in mitochondria, and finally contributes to neurodegeneration in AD [74,78,79]. Hence, the accumulation of intracellular calcium leads to neuronal death, and subsequent learning and memory impairment has been proposed [80].

The major limitation of this study is the sample size, which was unfortunately limited by budgetary constraints. Difficulties in the persuasion of patients or their caregivers to consent to the study were also occasionally encountered. With the limitation of the sample size in this study, it is clear that further investigation is required as there appear to be important revelations that may, in the future, provide much needed insight into

AD. Nevertheless, the study has addressed technical concerns regarding the problem of overfitting in the analysis of a limited sample size through cross-validation in *MSVM-RFE*.

## 6. Conclusions

This study presents preliminary findings on the differential miRNA expression in AD patients against normal controls in Malaysian subjects, providing some insight into the complex AD pathogenetic pathway. An integrative approach that combined a statistical approach, edgeR, and a two-step machine learning framework was conducted to support the analysis of data in this study. Three miRNAs, hsa-miR-6501-5p, hsa-miR-4433b-5p, and hsa-miR-143-3p, were identified as showing correlations between each other. Their biological roles in AD were indicated by predicting the target mRNAs of each respective miRNA, and pathway analysis suggested their relationships in the disease pathogenesis. Overall, the identified miRNAs, together with the target genes, were identified as being involved in pathways related to oxidative phosphorylation, mitochondrial dysfunction, and calcium-mediated signalling. Although the findings are consistent with the literature, they nonetheless represent the miRNA expression changes within a dataset characterized by a small sample size, and thus require further validation. This study provides further insight related to AD pathogenesis from the miRNA perspective, collected from the Malaysian population, which may potentially help in improving the diagnosis and treatment of this disease in the future.

**Supplementary Materials:** The following supporting information can be downloaded at: <https://www.mdpi.com/article/10.3390/app13053071/s1>, Table S1: Inclusion and exclusion criteria of selecting AD patients and normal controls; Table S2: Subject details and their corresponding ID used in this study; Sample preparation; Kits information.

**Author Contributions:** M.S.T.: Conceptualization; data curation; formal analysis, methodology; writing—original draft; writing—review and editing. P.-L.C.: Conceptualization; data curation; supervision; writing—review and editing. A.-V.C.: Conceptualization; data curation; supervision; writing—review and editing. L.-M.L.: Conceptualization; data curation; supervision; writing—review and editing. S.-W.C.: Conceptualization; data curation; methodology, supervision; writing—review and editing. All authors have read and agreed to the published version of the manuscript.

**Funding:** This work was supported in part by the Fundamental Research Grant Scheme (FRGS), Ministry of Higher Education Malaysia, project number FRGS/1/2019/SKK06/UM/02/5, and a UM International Collaboration Grant, project number ST041-2022. The funders had no role in study, design, data collection and analysis, decision to publish, or preparation of the manuscript.

**Institutional Review Board Statement:** The study protocol was approved by the Medical Research Ethics Committee, UMMC, with the approval number 2020114-9193.

**Informed Consent Statement:** Informed consent was obtained from all subjects involved in the study.

**Data Availability Statement:** All raw and processed sequencing data generated in this study have been submitted to the NCBI Gene Expression Omnibus (GEO) under accession number GSE224443 <https://www.ncbi.nlm.nih.gov/geo/query/acc.cgi?acc=GSE224443> (access on 2 February 2023).

**Conflicts of Interest:** The authors declare no conflict of interest.

## References

1. Wolk, D.A.; Dickerson, B.C. *Clinical Features and Diagnosis of Alzheimer Disease*; UpToDate: Waltham, MA, USA, 2016.
2. Abuelezz, N.Z.; Nasr, F.E.; AbdulKader, M.A.; Bassiouny, A.R.; Zaky, A. MicroRNAs as Potential Orchestrators of Alzheimer's Disease-Related Pathologies: Insights on Current Status and Future Possibilities. *Front. Aging Neurosci.* **2021**, *653*, 743573. [[CrossRef](#)] [[PubMed](#)]
3. Miya Shaik, M.; Tamargo, I.A.; Abubakar, M.B.; Kamal, M.A.; Greig, N.H.; Gan, S.H. The role of microRNAs in Alzheimer's disease and their therapeutic potentials. *Genes* **2018**, *9*, 174. [[CrossRef](#)] [[PubMed](#)]
4. Liu, Y.; Xu, Y.; Yu, M. MicroRNA-4722-5p and microRNA-615-3p serve as potential biomarkers for Alzheimer's disease. *Exp. Ther. Med.* **2022**, *23*, 1–10. [[CrossRef](#)] [[PubMed](#)]

5. Guévremont, D.; Tsui, H.; Knight, R.; Fowler, C.J.; Masters, C.L.; Martins, R.N.; Abraham, W.C.; Tate, W.P.; Cutfield, N.J.; Williams, J.M. Plasma microRNA vary in association with the progression of Alzheimer's disease. *Alzheimer's Dement. Diagn. Assess. Dis. Monit.* **2022**, *14*, e12251.
6. Zhang, W.; Zhang, G.; Gao, S. The potential diagnostic accuracy of circulating microRNAs for Alzheimer's disease: A meta-analysis. *Neurologia*, 2021; *in press*. [[CrossRef](#)]
7. Walgrave, H.; Zhou, L.; De Strooper, B.; Salta, E. The promise of microRNA-based therapies in Alzheimer's disease: Challenges and perspectives. *Mol. Neurodegener.* **2021**, *16*, 1–16. [[CrossRef](#)]
8. Angelucci, F.; Cechova, K.; Valis, M.; Kuca, K.; Zhang, B.; Hort, J. MicroRNAs in Alzheimer's disease: Diagnostic markers or therapeutic agents? *Front. Pharmacol.* **2019**, *10*, 665. [[CrossRef](#)]
9. Wu, H.Z.Y.; Thalamuthu, A.; Cheng, L.; Fowler, C.; Masters, C.L.; Sachdev, P.; Mather, K.A. Differential blood miRNA expression in brain amyloid imaging-defined Alzheimer's disease and controls. *Alzheimer's Res. Ther.* **2020**, *12*, 1–11. [[CrossRef](#)]
10. Kumar, S.; Reddy, P.H. Are circulating microRNAs peripheral biomarkers for Alzheimer's disease? *Biochim. Biophys. Acta (BBA)-Mol. Basis Dis.* **2016**, *1862*, 1617–1627. [[CrossRef](#)]
11. Liu, S.; Fan, M.; Zheng, Q.; Hao, S.; Yang, L.; Qi, C.; Ge, J.; Xia, Q. MicroRNAs in Alzheimer's disease: Potential diagnostic markers and therapeutic targets. *Biomed. Pharmacother.* **2022**, *148*, 112681. [[CrossRef](#)]
12. Fransquet, P.D.; Ryan, J. Micro RNA as a potential blood-based epigenetic biomarker for Alzheimer's disease. *Clin. Biochem.* **2018**, *58*, 5–14. [[CrossRef](#)] [[PubMed](#)]
13. Takousis, P.; Sadlon, A.; Schulz, J.; Wohlers, I.; Dobricic, V.; Middleton, L.; Lill, C.M.; Perneczky, R.; Bertram, L. Differential expression of microRNAs in Alzheimer's disease brain, blood, and cerebrospinal fluid. *Alzheimer's Dement.* **2019**, *15*, 1468–1477. [[CrossRef](#)] [[PubMed](#)]
14. Mahendran, N.; Vincent, P.D.R.; Srinivasan, K.; Chang, C.-Y. Improving the classification of Alzheimer's disease using hybrid gene selection pipeline and deep learning. *Front. Genet.* **2021**, *12*. [[CrossRef](#)]
15. Tan, M.S.; Cheah, P.-L.; Chin, A.-V.; Looi, L.-M.; Chang, S.-W. A review on omics-based biomarkers discovery for Alzheimer's disease from the bioinformatics perspectives: Statistical approach vs machine learning approach. *Comput. Biol. Med.* **2021**, *139*, 104947. [[CrossRef](#)] [[PubMed](#)]
16. Robles, J.A.; Qureshi, S.E.; Stephen, S.J.; Wilson, S.R.; Burden, C.J.; Taylor, J.M. Efficient experimental design and analysis strategies for the detection of differential expression using RNA-Sequencing. *BMC Genom.* **2012**, *13*, 484. [[CrossRef](#)] [[PubMed](#)]
17. Ziats, M.N.; Rennert, O.M. Identification of differentially expressed microRNAs across the developing human brain. *Mol. Psychiatry* **2014**, *19*, 848–852. [[CrossRef](#)] [[PubMed](#)]
18. Takahashi, Y.; Ueki, M.; Tamiya, G.; Ogishima, S.; Kinoshita, K.; Hozawa, A.; Minegishi, N.; Nagami, F.; Fukumoto, K.; Otsuka, K. Machine learning for effectively avoiding overfitting is a crucial strategy for the genetic prediction of polygenic psychiatric phenotypes. *Transl. Psychiatry* **2020**, *10*, 294. [[CrossRef](#)]
19. Bommert, A.; Welchowski, T.; Schmid, M.; Rahnenführer, J. Benchmark of filter methods for feature selection in high-dimensional gene expression survival data. *Brief. Bioinform.* **2022**, *23*, bbab354. [[CrossRef](#)]
20. Yuen, S.C.; Liang, X.; Zhu, H.; Jia, Y.; Leung, S.-w. Prediction of differentially expressed microRNAs in blood as potential biomarkers for Alzheimer's disease by meta-analysis and adaptive boosting ensemble learning. *Alzheimer's Res. Ther.* **2021**, *13*, 126. [[CrossRef](#)]
21. Zhao, Y.; Chen, X.; Yin, J. Adaptive boosting-based computational model for predicting potential miRNA-disease associations. *Bioinformatics* **2019**, *35*, 4730–4738. [[CrossRef](#)]
22. Lugli, G.; Cohen, A.M.; Bennett, D.A.; Shah, R.C.; Fields, C.J.; Hernandez, A.G.; Smalheiser, N.R. Plasma exosomal miRNAs in persons with and without Alzheimer disease: Altered expression and prospects for biomarkers. *PLoS ONE* **2015**, *10*, e0139233. [[CrossRef](#)] [[PubMed](#)]
23. Ludwig, N.; Fehlmann, T.; Kern, F.; Gogol, M.; Maetzler, W.; Deutscher, S.; Gurlit, S.; Schulte, C.; Von Thaler, A.-K.; Deuschle, C. Machine learning to detect Alzheimer's disease from circulating non-coding RNAs. *Genom. Proteom. Bioinform.* **2019**, *17*, 430–440. [[CrossRef](#)] [[PubMed](#)]
24. Martin, M. Cutadapt removes adapter sequences from high-throughput sequencing reads. *EMBnet J.* **2011**, *17*, 10–12. [[CrossRef](#)]
25. Langmead, B.; Salzberg, S.L. Fast gapped-read alignment with Bowtie 2. *Nat. Methods* **2012**, *9*, 357–359. [[CrossRef](#)]
26. Metpally, R.P.R.; Nasser, S.; Malenica, I.; Courtright, A.; Carlson, E.; Ghaffari, L.; Villa, S.; Tembe, W.; Van Keuren-Jensen, K. Comparison of analysis tools for miRNA high throughput sequencing using nerve crush as a model. *Front. Genet.* **2013**, *4*, 20. [[CrossRef](#)] [[PubMed](#)]
27. Robinson, M.D.; McCarthy, D.J.; Smyth, G.K. edgeR: A Bioconductor package for differential expression analysis of digital gene expression data. *Bioinformatics* **2010**, *26*, 139–140. [[CrossRef](#)]
28. Lang, M.; Binder, M.; Richter, J.; Schratz, P.; Pfisterer, F.; Coors, S.; Au, Q.; Casalicchio, G.; Kotthoff, L.; Bischl, B. mlr3: A modern object-oriented machine learning framework in R. *J. Open Source Softw.* **2019**, *4*, 1903. [[CrossRef](#)]
29. Zhou, X.; Tuck, D.P. MSVM-RFE: Extensions of SVM-RFE for multiclass gene selection on DNA microarray data. *Bioinformatics* **2007**, *23*, 1106–1114. [[CrossRef](#)]
30. Kohonen, T. *Self-Organizing Maps*; Springer Science & Business Media: Heidelberg, Germany, 2012; Volume 30.

31. Anke, Z.; Xinjian, Q.; Guojian, C. Clustering analysis of gene data based on PCA and SOM neural networks. In Proceedings of the 2014 Fifth International Conference on Intelligent Systems Design and Engineering Applications, Hunan, China, 15–16 June 2014; pp. 284–287.
32. Wehrens, R.; Buydens, L.M. Self-and super-organizing maps in R: The Kohonen package. *J. Stat. Softw.* **2007**, *21*, 1–19. [[CrossRef](#)]
33. Bro, R.; Smilde, A.K. Principal component analysis. *Anal. Methods* **2014**, *6*, 2812–2831. [[CrossRef](#)]
34. Jolliffe, I.T.; Cadima, J. Principal component analysis: A review and recent developments. *Philos. Trans. R. Soc. A Math. Phys. Eng. Sci.* **2016**, *374*, 20150202. [[CrossRef](#)] [[PubMed](#)]
35. Paraskevopoulou, M.D.; Georgakilas, G.; Kostoulas, N.; Vlachos, I.S.; Vergoulis, T.; Reczko, M.; Filippidis, C.; Dalamagas, T.; Hatzigeorgiou, A.G. DIANA-microT web server v5. 0: Service integration into miRNA functional analysis workflows. *Nucleic Acids Res.* **2013**, *41*, W169–W173. [[CrossRef](#)] [[PubMed](#)]
36. Vlachos, I.S.; Zagganas, K.; Paraskevopoulou, M.D.; Georgakilas, G.; Karagkouni, D.; Vergoulis, T.; Dalamagas, T.; Hatzigeorgiou, A.G. DIANA-miRPath v3. 0: Deciphering microRNA function with experimental support. *Nucleic Acids Res.* **2015**, *43*, W460–W466. [[CrossRef](#)] [[PubMed](#)]
37. Kanehisa, M.; Goto, S. KEGG: Kyoto encyclopedia of genes and genomes. *Nucleic Acids Res.* **2000**, *28*, 27–30. [[CrossRef](#)] [[PubMed](#)]
38. Young, M.D.; Wakefield, M.J.; Smyth, G.K.; Oshlack, A. Gene ontology analysis for RNA-seq: Accounting for selection bias. *Genome Biol.* **2010**, *11*, R14. [[CrossRef](#)]
39. Shannon, P.; Markiel, A.; Ozier, O.; Baliga, N.S.; Wang, J.T.; Ramage, D.; Amin, N.; Schwikowski, B.; Ideker, T. Cytoscape: A software environment for integrated models of biomolecular interaction networks. *Genome Res.* **2003**, *13*, 2498–2504. [[CrossRef](#)]
40. Ge, X.; Yao, T.; Zhang, C.; Wang, Q.; Wang, X.; Xu, L.-C. Human microRNA-4433 (hsa-miR-4443) Targets 18 Genes to be a Risk Factor of Neurodegenerative Diseases. *Curr. Alzheimer Res.* **2022**, *19*, 511–522.
41. Sproviero, D.; Gagliardi, S.; Zucca, S.; Arigoni, M.; Giannini, M.; Garofalo, M.; Olivero, M.; Dell’Orco, M.; Pansarasa, O.; Bernuzzi, S. Different miRNA profiles in plasma derived small and large extracellular vesicles from patients with neurodegenerative diseases. *Int. J. Mol. Sci.* **2021**, *22*, 2737. [[CrossRef](#)]
42. Peña-Bautista, C.; Álvarez-Sánchez, L.; Cañada-Martínez, A.J.; Baquero, M.; Cháfer-Pericás, C. Epigenomics and Lipidomics Integration in Alzheimer Disease: Pathways Involved in Early Stages. *Biomedicines* **2021**, *9*, 1812. [[CrossRef](#)]
43. Cheng, á.; Doecke, J.D.; Sharples, R.; Villemagne, V.L.; Fowler, C.J.; Rembach, A.; Martins, R.N.; Rowe, C.C.; Macaulay, S.L.; Masters, C.L. Prognostic serum miRNA biomarkers associated with Alzheimer’s disease shows concordance with neuropsychological and neuroimaging assessment. *Mol. Psychiatry* **2015**, *20*, 1188–1196. [[CrossRef](#)]
44. Hara, N.; Kikuchi, M.; Miyashita, A.; Hatsuta, H.; Saito, Y.; Kasuga, K.; Murayama, S.; Ikeuchi, T.; Kuwano, R. Serum microRNA miR-501-3p as a potential biomarker related to the progression of Alzheimer’s disease. *Acta Neuropathol. Commun.* **2017**, *5*, 10. [[CrossRef](#)]
45. Wang, L.; Shui, X.; Mei, Y.; Xia, Y.; Lan, G.; Hu, L.; Zhang, M.; Gan, C.-L.; Li, R.; Tian, Y. miR-143-3p Inhibits Aberrant Tau Phosphorylation and Amyloidogenic Processing of APP by Directly Targeting DAPK1 in Alzheimer’s Disease. *Int. J. Mol. Sci.* **2022**, *23*, 7992. [[CrossRef](#)] [[PubMed](#)]
46. Mayr, J.A.; Havlíčková, V.; Zimmermann, F.; Magler, I.; Kaplanova, V.; Ješina, P.; Pecinová, A.; Nůšková, H.; Koch, J.; Sperl, W. Mitochondrial ATP synthase deficiency due to a mutation in the ATP5E gene for the F1  $\epsilon$  subunit. *Hum. Mol. Genet.* **2010**, *19*, 3430–3439. [[CrossRef](#)] [[PubMed](#)]
47. Lunnon, K.; Keohane, A.; Pidsley, R.; Newhouse, S.; Riddoch-Contreras, J.; Thubron, E.B.; Devall, M.; Soininen, H.; Kłoszewska, I.; Mecocci, P. Mitochondrial genes are altered in blood early in Alzheimer’s disease. *Neurobiol. Aging* **2017**, *53*, 36–47. [[CrossRef](#)] [[PubMed](#)]
48. Chowdhury, U.N.; Islam, M.B.; Ahmad, S.; Moni, M.A. Network-based identification of genetic factors in ageing, lifestyle and type 2 diabetes that influence to the progression of Alzheimer’s disease. *Inform. Med. Unlocked* **2020**, *19*, 100309. [[CrossRef](#)]
49. Chiocco, M.J.; Zhu, X.; Walther, D.; Pletnikova, O.; Troncoso, J.C.; Uhl, G.R.; Liu, Q.-R. Fine mapping of calcineurin (PPP3CA) gene reveals novel alternative splicing patterns, association of 5’ UTR trinucleotide repeat with addiction vulnerability, and differential isoform expression in Alzheimer’s disease. *Subst. Use Misuse* **2010**, *45*, 1809–1826. [[CrossRef](#)]
50. Sadick, J.S.; Liddelow, S.A. Don’t forget astrocytes when targeting Alzheimer’s disease. *Br. J. Pharmacol.* **2019**, *176*, 3585–3598. [[CrossRef](#)]
51. Griswold, A.J.; Celis, K.; Bussies, P.L.; Rajabli, F.; Whitehead, P.L.; Hamilton-Nelson, K.L.; Beecham, G.W.; Dykxhoorn, D.M.; Nuytemans, K.; Wang, L. Increased APOE  $\epsilon$ 4 expression is associated with the difference in Alzheimer’s disease risk from diverse ancestral backgrounds. *Alzheimer’s Dement.* **2021**, *17*, 1179–1188. [[CrossRef](#)]
52. Morabito, S.; Miyoshi, E.; Michael, N.; Swarup, V. Integrative genomics approach identifies conserved transcriptomic networks in Alzheimer’s disease. *Hum. Mol. Genet.* **2020**, *29*, 2899–2919. [[CrossRef](#)]
53. Sesele, K.; Thanopoulou, K.; Paouri, E.; Tsefou, E.; Klinakis, A.; Georgopoulos, S. Conditional inactivation of nicastrin restricts amyloid deposition in an Alzheimer’s disease mouse model. *Aging Cell* **2013**, *12*, 1032–1040. [[CrossRef](#)]
54. Herrera-Rivero, M.; Hernández-Aguilar, M.E.; Aranda-Abreu, G.E. A strategy focused on MAPT, APP, NCSTN and BACE1 to build blood classifiers for Alzheimer’s disease. *J. Theor. Biol.* **2015**, *376*, 32–38. [[CrossRef](#)] [[PubMed](#)]
55. Andreoli, V.; De Marco, E.V.; Trecroci, F.; Cittadella, R.; Di Palma, G.; Gambardella, A. Potential involvement of GRIN2B encoding the NMDA receptor subunit NR2B in the spectrum of Alzheimer’s disease. *J. Neural Transm.* **2014**, *121*, 533–542. [[CrossRef](#)]

56. Wong, T.H.; van der Lee, S.J.; van Rooij, J.G.; Meeter, L.H.; Frick, P.; Melhem, S.; Seelaar, H.; Ikram, M.A.; Rozemuller, A.J.; Holstege, H. EIF2AK3 variants in Dutch patients with Alzheimer's disease. *Neurobiol. Aging* **2019**, *73*, 229.e11–229.e18. [[CrossRef](#)] [[PubMed](#)]
57. Liu, Q.-Y.; Yu, J.-T.; Miao, D.; Ma, X.-Y.; Wang, H.-F.; Wang, W.; Tan, L. An exploratory study on STX6, MOBP, MAPT, and EIF2AK3 and late-onset Alzheimer's disease. *Neurobiol. Aging* **2013**, *34*, 1519.e13–1519.e17. [[CrossRef](#)] [[PubMed](#)]
58. Cheng, J.; Liu, H.-P.; Lin, W.-Y.; Tsai, F.-J. Machine learning compensates fold-change method and highlights oxidative phosphorylation in the brain transcriptome of Alzheimer's disease. *Sci. Rep.* **2021**, *11*, 13704. [[CrossRef](#)]
59. Pinto, M.; Pickrell, A.M.; Fukui, H.; Moraes, C.T. Mitochondrial DNA damage in a mouse model of Alzheimer's disease decreases amyloid beta plaque formation. *Neurobiol. Aging* **2013**, *34*, 2399–2407. [[CrossRef](#)] [[PubMed](#)]
60. Randa, N.; Bora, E.; Ataman, E.; Öz, O.; Yener, G. Identification of PSEN1 and PSEN2 Gene Variants and Clinical Findings with the Literature. *Int. J. Neurodegener. Dis.* **2019**, *2*, 7.
61. Raut, S.; Patel, R.; Al-Ahmad, A.J. Presence of a mutation in PSEN1 or PSEN2 gene is associated with an impaired brain endothelial cell phenotype in vitro. *Fluids Barriers CNS* **2021**, *18*, 3. [[CrossRef](#)]
62. Du, Y.; Du, Y.; Zhang, Y.; Huang, Z.; Fu, M.; Li, J.; Pang, Y.; Lei, P.; Wang, Y.T.; Song, W. MKP-1 reduces A $\beta$  generation and alleviates cognitive impairments in Alzheimer's disease models. *Signal Transduct. Target. Ther.* **2019**, *4*, 58. [[CrossRef](#)]
63. Gee, M.S.; Son, S.H.; Jeon, S.H.; Do, J.; Kim, N.; Ju, Y.-J.; Lee, S.J.; Chung, E.K.; Inn, K.-S.; Kim, N.-J. A selective p38 $\alpha$ / $\beta$  MAPK inhibitor alleviates neuropathology and cognitive impairment, and modulates microglia function in 5XFAD mouse. *Alzheimer's Res. Ther.* **2020**, *12*, 1–18. [[CrossRef](#)]
64. Chen, C.; Liu, P.; Wang, J.; Yu, H.; Zhang, Z.; Liu, J.; Chen, X.; Zhu, F.; Yang, X. Dauricine attenuates spatial memory impairment and alzheimer-like pathologies by enhancing mitochondrial function in a mouse model of Alzheimer's disease. *Front. Cell Dev. Biol.* **2021**, *8*, 624339. [[CrossRef](#)] [[PubMed](#)]
65. Adav, S.S.; Park, J.E.; Sze, S.K. Quantitative profiling brain proteomes revealed mitochondrial dysfunction in Alzheimer's disease. *Mol. Brain* **2019**, *12*, 8. [[CrossRef](#)]
66. Gong, S.; Su, B.B.; Tovar, H.; Mao, C.; Gonzalez, V.; Liu, Y.; Lu, Y.; Wang, K.-S.; Xu, C. Polymorphisms within RYR3 gene are associated with risk and age at onset of hypertension, diabetes, and Alzheimer's disease. *Am. J. Hypertens.* **2018**, *31*, 818–826. [[CrossRef](#)] [[PubMed](#)]
67. Del Prete, D.; Checler, F.; Chami, M. Ryanodine receptors: Physiological function and deregulation in Alzheimer disease. *Mol. Neurodegener.* **2014**, *9*, 21. [[CrossRef](#)] [[PubMed](#)]
68. Supnet, C.; Noonan, C.; Richard, K.; Bradley, J.; Mayne, M. Up-regulation of the type 3 ryanodine receptor is neuroprotective in the TgCRND8 mouse model of Alzheimer's disease. *J. Neurochem.* **2010**, *112*, 356–365. [[CrossRef](#)]
69. Das, B.; Yan, R. Role of BACE1 in Alzheimer's synaptic function. *Transl. Neurodegener.* **2017**, *6*, 1–8. [[CrossRef](#)]
70. Cervellati, C.; Valacchi, G.; Zuliani, G. BACE1 role in Alzheimer's disease and other dementias: From the theory to the practice. *Neural Regen. Res.* **2021**, *16*, 2407. [[CrossRef](#)]
71. McDade, E.; Voytyuk, I.; Aisen, P.; Bateman, R.J.; Carrillo, M.C.; De Strooper, B.; Haass, C.; Reiman, E.M.; Sperling, R.; Tariot, P.N. The case for low-level BACE1 inhibition for the prevention of Alzheimer disease. *Nat. Rev. Neurol.* **2021**, *17*, 703–714. [[CrossRef](#)]
72. Bi, R.; Zhang, W.; Zhang, D.-F.; Xu, M.; Fan, Y.; Hu, Q.-X.; Jiang, H.-Y.; Tan, L.; Li, T.; Fang, Y. Genetic association of the cytochrome c oxidase-related genes with Alzheimer's disease in Han Chinese. *Neuropsychopharmacology* **2018**, *43*, 2264–2276. [[CrossRef](#)]
73. Wilkins, H.M.; Koppel, S.J.; Bothwell, R.; Mahnken, J.; Burns, J.M.; Swerdlow, R.H. Platelet cytochrome oxidase and citrate synthase activities in APOE  $\epsilon$ 4 carrier and non-carrier Alzheimer's disease patients. *Redox Biol.* **2017**, *12*, 828–832. [[CrossRef](#)]
74. Alldred, M.J.; Lee, S.H.; Stutzmann, G.E.; Ginsberg, S.D. Oxidative phosphorylation is dysregulated within the basocortical circuit in a 6-month old mouse model of down syndrome and alzheimer's disease. *Front. Aging Neurosci.* **2021**, *13*, 484. [[CrossRef](#)]
75. Misrani, A.; Tabassum, S.; Yang, L. Mitochondrial dysfunction and oxidative stress in Alzheimer's disease. *Front. Aging Neurosci.* **2021**, *13*, 617588. [[CrossRef](#)] [[PubMed](#)]
76. Bell, S.M.; Barnes, K.; De Marco, M.; Shaw, P.J.; Ferraiuolo, L.; Blackburn, D.J.; Venneri, A.; Mortiboys, H. Mitochondrial dysfunction in Alzheimer's disease: A biomarker of the future? *Biomedicines* **2021**, *9*, 63. [[CrossRef](#)] [[PubMed](#)]
77. Wang, W.; Zhao, F.; Ma, X.; Perry, G.; Zhu, X. Mitochondria dysfunction in the pathogenesis of Alzheimer's disease: Recent advances. *Mol. Neurodegener.* **2020**, *15*, 1–22. [[CrossRef](#)] [[PubMed](#)]
78. Liu, L.; Gao, H.; Zaikin, A.; Chen, S. Unraveling A $\beta$ -mediated multi-pathway calcium dynamics in astrocytes: Implications for Alzheimer's disease treatment from simulations. *Front. Physiol.* **2021**, *12*, 1918. [[CrossRef](#)]
79. Popugaeva, E.; Pchitskaya, E.; Bezprozvanny, I. Dysregulation of intracellular calcium signaling in Alzheimer's disease. *Antioxid. Redox Signal.* **2018**, *29*, 1176–1188. [[CrossRef](#)]
80. Workgroup, A.S.A.C.H.; Khachaturian, Z.S. Calcium hypothesis of Alzheimer's disease and brain aging: A framework for integrating new evidence into a comprehensive theory of pathogenesis. *Alzheimer's Dement.* **2017**, *13*, 178–182.e17.

**Disclaimer/Publisher's Note:** The statements, opinions and data contained in all publications are solely those of the individual author(s) and contributor(s) and not of MDPI and/or the editor(s). MDPI and/or the editor(s) disclaim responsibility for any injury to people or property resulting from any ideas, methods, instructions or products referred to in the content.